

Article

Impact of Radial Lands on the Reduction of Torque/Force Generation of a Heat-Treated Nickel-Titanium Rotary Instrument

Taro Nakatsukasa, Arata Ebihara *, Moe Sandar Kyaw, Satoshi Omori, Hayate Unno, Shunsuke Kimura, Keiichiro Maki and Takashi Okiji 

Department of Pulp Biology and Endodontics, Division of Oral Health Sciences, Graduate School of Medical and Dental Sciences, Tokyo Medical and Dental University (TMDU), 1-5-45 Yushima, Bunkyo-ku, Tokyo 113 8549, Japan; t.nakatsukasa.endo@tmd.ac.jp (T.N.); kyawendo@tmd.ac.jp (M.S.K.); s.omori.endo@tmd.ac.jp (S.O.); h.unno.endo@tmd.ac.jp (H.U.); s.kimura.endo@tmd.ac.jp (S.K.); k.maki.endo@tmd.ac.jp (K.M.); t.okiji.endo@tmd.ac.jp (T.O.)

* Correspondence: a.ebihara.endo@tmd.ac.jp; Tel.: +81-3-580-5494

Abstract: This study investigated the impact of a one-sided radial-landed cross-sectional design of a heat-treated nickel-titanium rotary instrument (JIZAI, MANI, Japan; JZ) on torque/force generation and canal-shaping ability, using an experimental non-landed instrument (non-landed JZ) for comparison. Both instruments had tip sizes of 25 and 0.04 or 0.06 taper and were similar in metallurgy and geometry, except for the presence/absence of a radial land. Twenty J-shaped simulated resin canals were instrumented in a two-instrument single-length sequence using an automated root canal instrumentation device with a torque/force analyzing unit. Pre- and post-instrumentation images of the resin canals were analyzed for canal-centering ability at 0–3 mm from the apex. The mean centering ratio was not significantly different between JZ and non-landed JZ ($p > 0.05$). In the 2nd instrumentation, JZ showed a significantly smaller torque compared with the non-landed JZ ($p < 0.05$). Regardless of instrumentation sequence, JZ showed a significantly smaller maximum upward force, representing screw-in force ($p < 0.05$), and a larger maximum downward force ($p < 0.05$) than the non-landed JZ. JZ generated smaller screw-in forces and had similar canal-centering ability compared with the non-landed JZ.

Keywords: canal-centering ability; nickel-titanium rotary instrument; radial land; screw-in force; torque



Citation: Nakatsukasa, T.; Ebihara, A.; Kyaw, M.S.; Omori, S.; Unno, H.; Kimura, S.; Maki, K.; Okiji, T. Impact of Radial Lands on the Reduction of Torque/Force Generation of a Heat-Treated Nickel-Titanium Rotary Instrument. *Appl. Sci.* **2022**, *12*, 2620. <https://doi.org/10.3390/app12052620>

Academic Editor: Gianluca Gambarini

Received: 5 February 2022

Accepted: 28 February 2022

Published: 3 March 2022

Publisher's Note: MDPI stays neutral with regard to jurisdictional claims in published maps and institutional affiliations.



Copyright: © 2022 by the authors. Licensee MDPI, Basel, Switzerland. This article is an open access article distributed under the terms and conditions of the Creative Commons Attribution (CC BY) license (<https://creativecommons.org/licenses/by/4.0/>).

1. Introduction

Nickel-titanium (NiTi) rotary instruments are considered suitable for preparing curved root canals because of their higher flexibility [1] and superior canal-centering ability [2] compared with stainless steel files. However, intracanal fracture of NiTi rotary instruments is a problem that has not yet been fully resolved [3]. Tight binding of a rotating instrument with the canal wall may induce torsional overload and, thus, is considered as a cause of the fracture [4]. Moreover, the binding may produce a pulling force toward the root apex on the rotating instrument due to the helical design of the flutes. This phenomenon, termed the screw-in effect, may cause instantaneous engagement of the instrument giving rise to sudden torsional fracture [5]. The screw-in effect may also cause over-instrumentation, which could induce postoperative pain [6] and increase the risk of apical crack formation [7]. The screw-in tendency of NiTi rotary instruments is associated with their geometry; instruments with an active cutting edge and short pitch length may thread into the canal wall leading to a greater tendency to screw-in [8,9]. In addition, pecking motion with higher pecking speed [10] and shorter pecking depth [11], and reciprocal rotation [12,13] reduce the screw-in force.

Heat treatment of NiTi alloys changes their phase transformation temperatures, leading to generation of soft and ductile R-phase and martensite phase at room or body

temperature [14,15]. Thus, contemporary heat-treated NiTi instruments exhibit a significant improvement in flexibility, cyclic fatigue resistance [16,17] and canal-centering ability [18] compared with conventional NiTi instruments. The heat-treated instruments are reported to produce less screw-in forces compared with those manufactured from conventional alloys [13].

Radial land is a smooth cutting surface between the flutes of a rotary instrument. Radial land scrapes the canal wall with a planing action and is believed to allow the instrument to remain centered in the canal space, leading to safer and less deviated instrumentation [19]. A radial-landed design was incorporated in several early generations of NiTi rotary instruments, such as ProFile (Dentsply Sirona, Ballaigues, Switzerland), which has three landed areas in a cross-section. ProFile produces significantly less transportation compared with non-landed instruments with actively cutting blades [20,21] and generates smaller screw-in force compared with non-landed instruments [9]. Nevertheless, later, NiTi rotary systems were designed usually with actively cut blades without radial lands to increase the cutting efficiency [19], although this could give rise to a certain risk of preparation errors such as canal straightening [20,21].

JIZAI (MANI, Utsunomiya, Japan; JZ) is a recently developed NiTi rotary system fabricated from a proprietary heat-treated NiTi alloy. JZ has a unique quasi-rectangular cross-sectional shape in which a radial land is provided on one of the short sides (Figure 1A). JZ (#25/.06 taper) is reported to generate a smaller screw-in force and shows better canal-centering ability compared with HyFlex EDM OneFile (#25/.08 taper at the tip; Coltene-Whaledent, Allstatten, Switzerland) [22]. The one-side radial-landed cross-sectional design of JZ can be assumed as a factor impacting these findings.

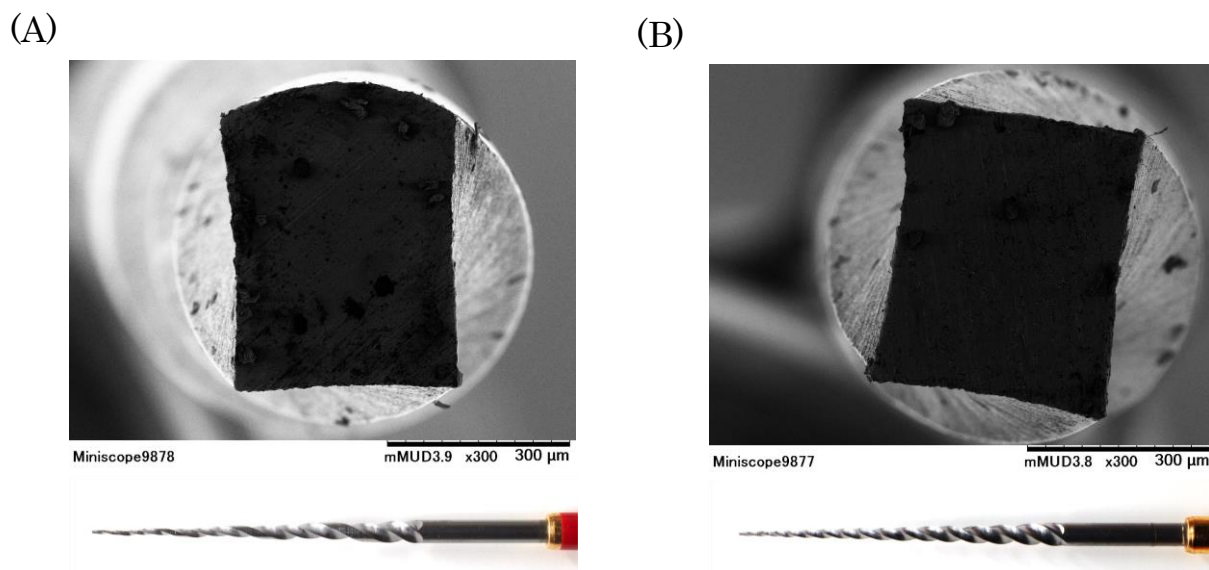


Figure 1. Cross-sectional shape and cutting portion of the JIZAI instrument (A) and the non-landed experimental instrument (B).

Information on the effect of design features of NiTi rotary instruments on their canal-shaping ability [23] and screw-in force generation [9,13,22] has been gained through numerous laboratory studies using commercially available instruments. However, most of these studies have a major drawback, which is the inability to eliminate several confounding parameters other than a single variable of interest, resulting from the difference in multiple parameters among the brands being tested. Thus, some studies have compared instruments with the same geometry but different heat-treatment [22,24,25]. In this regard, to the best of our knowledge, no studies to date have definitively proven the impact of the radial land on the shaping performance of NiTi rotary instruments. Taking these concerns into account, we designed this study to determine the effect of the one-sided radial-landed design of JZ on the torque/force generation and canal-shaping ability, under a condition where the

impact of other influencing factors, such as heat-treatment, taper, pitch length and instrumentation protocol, is minimized. To achieve this, we employed an experimental NiTi rotary instrument (termed non-landed JZ; Figure 1B), which is a non-landed counterpart of JZ with identical metallurgy and almost the same geometrical features. The null hypothesis was that JZ and non-landed JZ do not differ in terms of torque and vertical force generation and canal-shaping ability.

2. Materials and Methods

2.1. Test Instruments

JZ and non-landed JZ of the tip size #25 and 0.04 or 0.06 taper were used. Both instruments were made of the same heat-treated alloy, and the cutting portion consisted of 16 threads. The cross-section of JZ is a quasi-rectangle with radial land on one of the short sides, and that of the non-landed JZ is a rectangle without radial lands.

2.2. Sample Size Calculation

G*Power 3.1.9 (Universität Kiel, Kiel, Germany) was used to calculate the sample size. An effect size of 0.7, study power of 95%, and alpha-type error of 0.05, were considered based on our previous studies [10,22]. The sample size was estimated to be at least 8 in each group.

2.3. Evaluation of Torque and Vertical Force

Twenty J-shaped simulated resin root canal models (Endo Training Bloc, Dentsply Sirona) were used. Coronal flaring was performed to a depth of 4 mm from the apex with a NiTi rotary instrument (ProTaper SX, Dentsply Sirona, Ballaigues, Switzerland), and the glide path was established manually with #10, #15, and #20 stainless steel K-files (Zipperer, Munich, Germany). The models were then randomly assigned to two test instruments, i.e., JZ and non-landed JZ ($n = 10$ each).

Each model was instrumented using an automated root canal instrumentation device, and torque and force generated during the instrumentation were monitored with a torque/force measuring unit attached to the root canal instrumentation device (Figure 2), as described previously [12]. Briefly, the device consisted of a test stand with a moving stage (MX2-500N; IMADA, Aichi, Japan), and the torque/force measuring unit consisting of a load cell (LUX-B-ID; Kyowa, Tokyo, Japan; rated capacity, ± 50 N; nonlinearity, within $\pm 0.15\%$ of rated output) and strain gauges (KFG-2-120-D31-11; Kyowa; foil type; strain limits at room temperature, approximately 5%) was connected to the model to measure the apical/coronal vertical loads and clockwise torque, respectively. A liner correlation has been confirmed between the distortion values measured by the strain gauges and torque values [12]. An endodontic motor (J Morita, Kyoto, Japan) attached to the moving stage of the stand was programmed to repeat an up-and-down movement at 50 mm/min for 2 and 1 s in the apical and coronal directions, respectively [10]. The maximum torque and force values were evaluated.

Instrumentation was performed using a two-instrument sequence following the manufacturers' recommendations for curved canals, and size #25/0.04 and #25/0.06 taper instruments were used sequentially at a rotational speed of 500 rpm. In the first sequence (#25/0.04 taper), the canal was instrumented to 2 mm short of the apex and then to the full working length. In the second sequence (#25/0.06 taper), the canal was instrumented sequentially to 2 and 1 mm short of the apex and finally to the full working length. As a lubricant, RC-Prep (Premier, Plymouth Meeting, PA, USA) was used [9]. Before each instrument change, canal patency was checked with a #10 K-file followed by canal irrigation with 1 mL of distilled water. All instruments used for instrumentation were examined with a surgical operating microscope (OPMI pico, Carl Zeiss, Gottingen, Germany) at $\times 21.3$ magnification for any possible defect or distortion (plastic deformation).

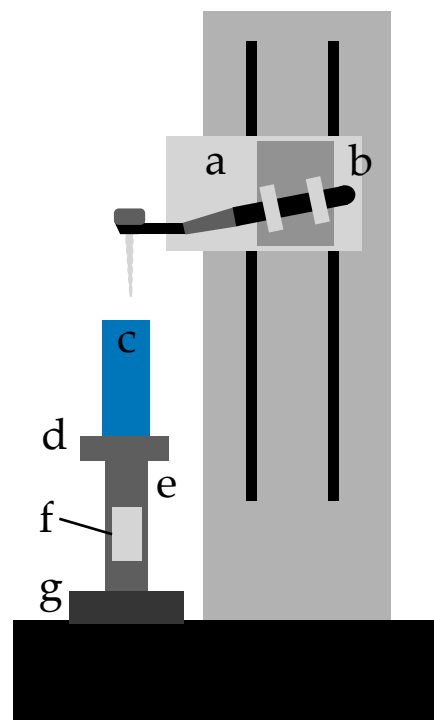


Figure 2. Automated root canal instrumentation device with a torque/force analyzing unit. (a) moving stage; (b) endodontic motor; (c) canal model; (d) metal stage; (e) metal cylinder; (f) strain gauge; (g) load cell. The metal stage (d), on which a canal model (c) was fixed, was connected to the load cell for force measurement (g) with a metal cylinder (e). The metal cylinder had a flattened portion in its center, where the strain gauges for torque measurement (f) were adhered.

2.4. Canal-Centering Ability

Measurements were performed using image analyzing software (Photoshop 7.0, Adobe Systems, San Jose, CA, USA), as described previously [10]. Briefly, following superimposition of pre- and post-instrumentation images of the root canal models, taken with a digital microscope (VH-8000; Keyence, Osaka, Japan), measuring points were determined at 0, 0.5, 1, 2, and 3 mm levels from the apex. The canal-centering ratio was calculated as $(A-B)/C$, where A and B represent the amount of resin removed from the outer side and inner side, respectively, and C represents post-instrumentation canal diameter [10]. In this formula, a value of zero indicates perfect centering.

2.5. Statistical Analysis

The normality and homogeneity of variance of the data were verified using the Shapiro–Wilk test and the Levene F test, respectively. The data were then analyzed using two-way repeated-measures analysis of variance (ANOVA), and the main effect and interaction of the independent variables were confirmed. If both were significant, the simple main effect was tested, and if it was significant, all pairwise comparisons were made using the Bonferroni test ($\alpha = 0.05$). All the statistical analysis was conducted using SPSS Statistics (version 23.0; IBM, Armonk, NY, USA).

3. Results

3.1. Canal-Centering Ratio

According to two-way ANOVA, “instrument” and “measuring point” influenced the centering ratio ($p < 0.05$) with significant interactions ($p < 0.05$).

As shown in Figure 3, the mean centering ratio at 0, 0.5, 1, 2, and 3 mm from the apex did not show a significant difference between JZ and the non-landed JZ ($p > 0.05$).

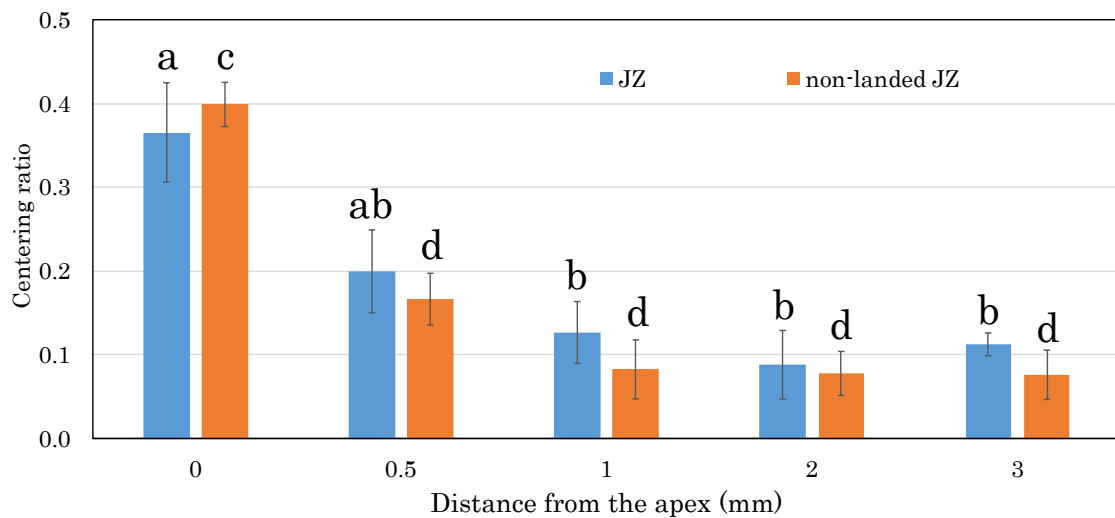


Figure 3. Canal-centering ratio at 0, 0.5, 1, 2, and 3 mm from the apex. Data represent the mean and standard deviation ($n = 10$). JZ and the non-landed JZ are not significantly different at each measuring point ($p > 0.05$). Different lowercase letters indicate the centering ratio values are significantly different within the same instrument ($p < 0.05$).

3.2. Torque and Vertical Force

According to two-way ANOVA, “instrument” and “instrumentation sequence (1st or 2nd)” influenced the maximum torque and vertical force values ($p < 0.05$). There was a significant interaction between the two factors ($p < 0.05$).

The maximum torque in the 1st instrumentation was not significantly different between the two instruments ($p > 0.05$; Figure 4). In the 2nd instrumentation, JZ showed a significantly smaller torque compared with the non-landed JZ ($p < 0.05$; Figure 4).

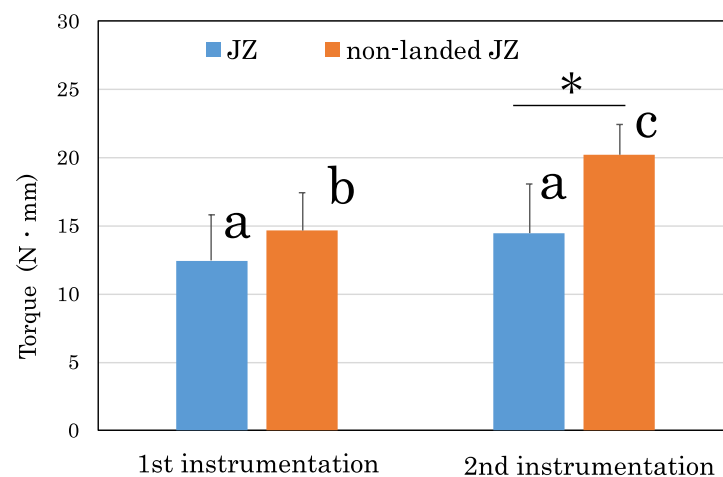


Figure 4. Maximum values of torque during root canal instrumentation. Data represent the mean and standard deviation ($n = 10$). * $p < 0.05$ within the same instrumentation sequence. Different lowercase letters are significantly different within the same instrument ($p < 0.05$).

Regardless of the instrumentation sequence, JZ showed significantly smaller maximum upward force values ($p < 0.05$; Figure 5A) and larger maximum downward force values ($p < 0.05$; Figure 5B) compared with the non-landed JZ.

No instrument deformation or fracture occurred during the experiment.

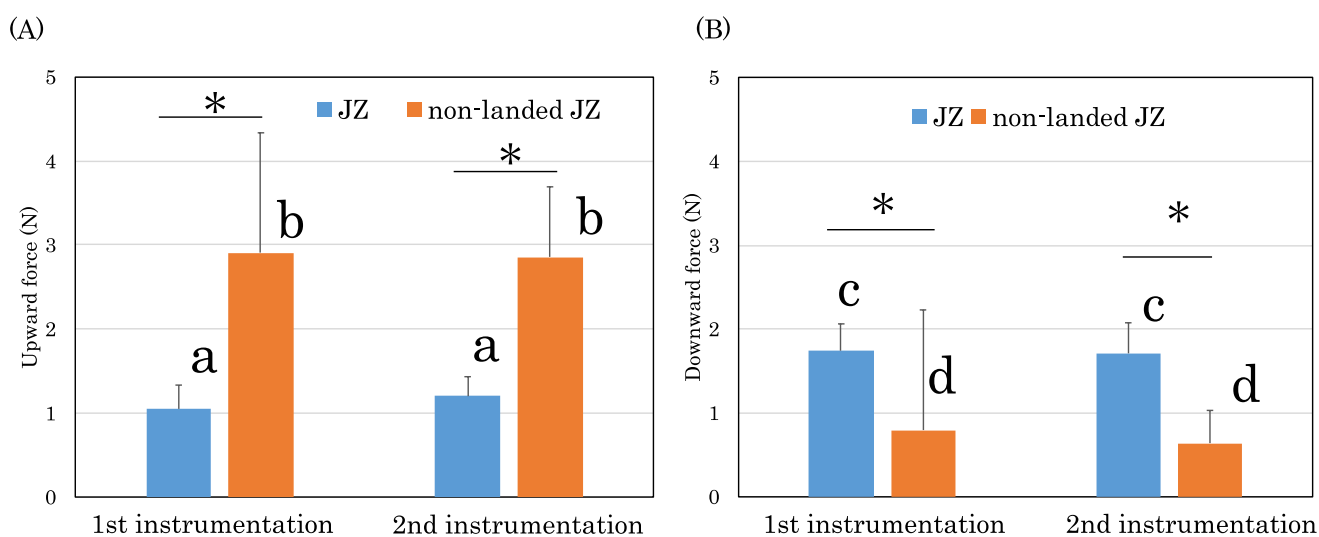


Figure 5. Maximum values of upward force (A) and downward force (B) during root canal instrumentation. Data represent the mean and standard deviation ($n = 10$). * $p < 0.05$ within the same instrumentation sequence. Different lowercase letters are significantly different within the same instrument ($p < 0.05$).

4. Discussion

This study analyzed the effect of radial-landed geometry of NiTi rotary instruments on canal-centering ability and torque/force generation, both of which play a crucial role in determining the clinical performance of these instruments [26]. In this study, impact of metallurgic and geometrical factors, except for the presence/absence of a radial land, was made as minimal as possible by using the non-landed JZ as the control. The use of an automated root canal instrumentation device may have contributed to a reproducible assessment while avoiding human intervention. An up-and-down speed of 50 mm/min was set based on a previous study [10]. The results demonstrated that the two instruments did not differ in their canal-centering ability, but JZ exhibited a significantly smaller upward force (screw-in force) and a larger downward force compared with its counterpart (non-landed JZ). Thus, the null hypothesis is partially rejected.

Simulated resin canals were employed in the present study to standardize the analysis by excluding morphological differences inherent in natural root canals [27]. In particular, simulated resin canals are more suitable for providing standardized evaluation with direct visual comparison of the centering ratio compared with natural root canals [18,28]. Thus, many studies have used resin canals as a valid alternative to natural root canals to investigate torque/force generation [29,30] and canal transportation [31,32] during root canal instrumentation. However, the use of simulated resin canals has limitations because their physical properties such as hardness that differs from those of real teeth [33]. Resin canals are softer and have a smoother surface texture than dentin and may require less force to cut [27]; nevertheless, instrumentation in resin canals may generate larger stress than in human root dentin because rotary instruments may become entangled in shavings and heat-softened resin [34]. In this regard, future studies using extracted teeth may provide more clinically relevant implications.

JZ is made of a heat-treated NiTi alloy, and the manufacturer claims that JZ contains a considerable amount of R-phase at room and body temperatures, although the phase transformation temperature of JZ has not yet been reported. JZ shows improvements in terms of flexibility, cyclic fatigue resistance, and canal-centering ability compared with a non-heat-treated instrument with identical geometry [22], which agrees with the findings of several studies showing that heat treatment improves the mechanical properties of NiTi rotary instruments [15–18,35].

Radial lands are believed to prevent deviation of canal preparation from the curvature by their passively cutting nature that helps keeping a rotating instrument centered in the canal [36]. In fact, some studies have demonstrated that landed instruments such as ProFile [20,21] and JZ [22] exhibit a better ability to maintain canal curvature compared with non-landed instruments. This study, however, failed to demonstrate any significant difference between JZ and the non-landed JZ in terms of canal-centering ability, which could be due to the increased flexibility of these instruments resulting from the heat treatment [22]. Since flexible instruments show better ability to follow the canal curvature [18], it seems reasonable to suppose that the flexibility of the heat-treated alloy compensated for the canal-straightening tendency of the non-landed instrument. Thus, in heat-treated flexible instruments, geometric features other than radial lands, such as the taper [31] and core diameter [37], may have greater contribution to the degree of canal straightening.

JZ generated a smaller torque compared with the non-landed JZ in the 2nd instrumentation, which is in line with the findings of previous studies showing that landed instruments (ProFile) produce a smaller torque compared with non-landed instruments (ProTaper, Dentsply Sirona) [38,39]. These findings can be attributed to the presence of sharp cutting edges in the non-landed instruments and supports the view that radial land contributes to the decrease in torsional load during rotary instrumentation.

In the 1st and 2nd instrumentation, JZ showed a significantly smaller upward force, representing the screw-in force, compared with the non-landed JZ. This is in agreement with a previous study showing that ProFile instruments generate smaller screw-in force compared with non-landed instruments such as ProTaper [9]. Thus, the present findings corroborate the notion that instruments with active cutting edges tend to thread into the canal wall and exhibit a greater tendency to screw-in compared with passive landed instruments [9].

Conversely, JZ showed a significantly larger downward force than the non-landed JZ, which is in line with the finding that ProFile generates a greater downward force compared with ProTaper [38]. Because downward forces are largely a function of the apically directed feed of an instrument, the difference between the two instruments could be explained by the different screw-in tendencies that could have released the downward force in the opposite direction.

The difference in geometry may influence the mechanical properties and shaping ability of NiTi rotary instruments [22,34]. Thus, the incorporation of radial lands could alter some characteristics of the instruments, such as bending property, cutting efficiency, debris-removing capacity, and pattern of stress distribution, even though geometric features other than radial land were as identical as possible. The effect of these “secondary” influencing factors could not be ruled out on the difference in stress generation between JZ and the non-landed JZ.

5. Conclusions

Under standardized conditions using the automated instrumentation and torque/force analyzing device, a one-side-landed NiTi rotary instrument (JZ) generated smaller screw-in forces and similar canal-centering ability compared with its non-landed counterpart (non-landed JZ).

Author Contributions: Conceptualization, T.N., A.E., M.S.K., S.O., H.U., S.K., K.M. and T.O.; methodology, T.N., M.S.K., S.O. and H.U.; sample testing, T.N.; date and statistical analysis, T.N., S.K. and K.M.; writing—original draft preparation, T.N., A.E. and T.O.; writing—review and editing, T.N., A.E. and T.O.; supervision and project administration, A.E. and T.O.; funding acquisition, A.E. All authors have read and agreed to the published version of the manuscript.

Funding: This research was funded by a Grant-in-Aid for Scientific Research (grant no. 19K18987) from the Japan Society for the Promotion of Science.

Institutional Review Board Statement: Not applicable.

Informed Consent Statement: Not applicable.

Data Availability Statement: Data supporting reported results can be obtained from T.N.

Acknowledgments: The authors thank MANI for supplying the NiTi rotary instruments used in the experiment.

Conflicts of Interest: The authors declare no conflict of interest.

References

1. Gambill, J.M.; Alder, M.; del Rio, C.E. Comparison of Nickel-Titanium and Stainless Steel Hand-File Instrumentation Using Computed Tomography. *J. Endod.* **1996**, *22*, 369–375. [[CrossRef](#)]
2. Glossen, C.R.; Haller, R.H.; Dove, S.B.; del Rio, C.E. A Comparison of Root Canal Preparations Using Ni-Ti Hand, Ni-Ti Engine-Driven, and K-Flex Endodontic Instruments. *J. Endod.* **1995**, *21*, 146–151. [[CrossRef](#)]
3. McGuigan, M.B.; Louca, C.; Duncan, H.F. Endodontic Instrument Fracture: Causes and Prevention. *Br. Dent. J.* **2013**, *214*, 341–348. [[CrossRef](#)]
4. Park, S.Y.; Cheung, G.S.; Yum, J.; Hur, B.; Park, J.K.; Kim, H.C. Dynamic Torsional Resistance of Nickel-Titanium Rotary Instruments. *J. Endod.* **2010**, *36*, 1200–1204. [[CrossRef](#)]
5. Parashos, P.; Gordon, I.; Messer, H.H. Factors Influencing Defects of Rotary Nickel-Titanium Endodontic Instruments After Clinical Use. *J. Endod.* **2004**, *30*, 722–725. [[CrossRef](#)]
6. Shubham, S.; Nepal, M.; Mishra, R.; Dutta, K. Influence of Maintaining Apical Patency In Post-Endodontic Pain. *BMC Oral Health* **2021**, *21*, 1–10. [[CrossRef](#)]
7. Adorno, C.G.; Yoshioka, T.; Suda, H. Crack Initiation on the Apical Root Surface Caused by Three Different Nickel-Titanium Rotary Files at Different Working Lengths. *J. Endod.* **2011**, *37*, 522–525. [[CrossRef](#)]
8. Diemer, F.; Calas, P. Effect of Pitch Length on the Behavior of Rotary Triple Helix Root Canal Instruments. *J. Endod.* **2004**, *30*, 716–718. [[CrossRef](#)]
9. Ha, J.H.; Jin, M.U.; Kim, Y.K.; Kim, S.K. Comparison of Screw-In Effect for Several Nickel-Titanium Rotary Instruments in Simulated Resin Root Canal. *J. Korean Acad. Conserv. Dent.* **2010**, *35*, 267–272. [[CrossRef](#)]
10. Maki, K.; Ebihara, A.; Kimura, S.; Nishijo, M.; Tokita, D.; Okiji, T. Effect of Different Speeds of Up-and-down Motion on Canal Centering Ability and Vertical Force and Torque Generation of Nickel-titanium Rotary Instruments. *J. Endod.* **2019**, *45*, 68–72.e1. [[CrossRef](#)]
11. Ha, J.-H.; Kwak, S.W.; Sigurdsson, A.; Chang, S.W.; Kim, S.K.; Kim, H.-C. Stress Generation during Pecking Motion of Rotary Nickel-titanium Instruments with Different Pecking Depth. *J. Endod.* **2017**, *43*, 1688–1691. [[CrossRef](#)] [[PubMed](#)]
12. Tokita, D.; Ebihara, A.; Nishijo, M.; Miyara, K.; Okiji, T. Dynamic Torque and Vertical Force Analysis during Nickel-titanium Rotary Root Canal Preparation with Different Modes of Reciprocal Rotation. *J. Endod.* **2017**, *43*, 1706–1710. [[CrossRef](#)] [[PubMed](#)]
13. Kwak, S.W.; Lee, C.-J.; Kim, S.K.; Kim, H.-C.; Ha, J.-H. Comparison of Screw-In Forces during Movement of Endodontic Files with Different Geometries, Alloys, and Kinetics. *Materials* **2019**, *12*, 1506. [[CrossRef](#)]
14. Shim, K.S.; Oh, S.; Kum, K.; Kim, Y.C.; Jee, K.K.; Chang, S.W. Mechanical and Metallurgical Properties of Various Nickel-Titanium Rotary Instruments. *Biomed. Res. Int.* **2017**, *2017*, 4528601. [[CrossRef](#)]
15. Shen, Y.; Zhou, H.M.; Zheng, Y.F.; Peng, B.; Haapasalo, M. Current Challenges and Concepts of the Thermomechanical Treatment of Nickel-Titanium Instruments. *J. Endod.* **2013**, *39*, 163–172. [[CrossRef](#)]
16. Zupanc, J.; Vahdat-Pajouh, N.; Schäfer, E. New Thermomechanically Treated NiTi Alloys—A Review. *Int. Endod. J.* **2018**, *51*, 1088–1103. [[CrossRef](#)]
17. Lopes, H.P.; Gambarra-Soares, T.; Elias, C.N.; Siqueira, J.F., Jr.; Inojosa, I.F.; Lopes, W.S.; Vieira, V.T. Comparison of the Mechanical Properties of Rotary Instruments Made of Conventional Nickel-Titanium Wire, M-Wire, or Nickel-Titanium Alloy in R-phase. *J. Endod.* **2013**, *39*, 516–520. [[CrossRef](#)]
18. Burroughs, J.R.; Bergeron, B.E.; Roberts, M.D.; Hagan, J.L.; Himel, V.T. Shaping Ability of Three Nickel-Titanium Endodontic File Systems in Simulated S-shaped Root Canals. *J. Endod.* **2012**, *38*, 1618–1621. [[CrossRef](#)]
19. Haapasalo, M.; Shen, Y. Evolution of Nickel-Titanium Instruments: From Past to Future. *Endod. Top.* **2013**, *29*, 3–17. [[CrossRef](#)]
20. Al-Sudani, D.; Al-Shahrani, S. A Comparison of the Canal Centering Ability of ProFile, K3, and RaCe Nickel Titanium Rotary Systems. *J. Endod.* **2006**, *32*, 1198–1201. [[CrossRef](#)]
21. Çelik, G.; Maden, M.; Savgat, A.; Orhan, A. Shaping Ability of the ProFile 25/0.06 and ProTaper F2 in Rotary Motion, and Reciproc in Simulated Canals. *PeerJ* **2018**, *6*, e6109. [[CrossRef](#)] [[PubMed](#)]
22. Nakatsukasa, T.; Ebihara, A.; Kimura, S.; Maki, K.; Nishijo, M.; Tokita, D.; Okiji, T. Comparative Evaluation of Mechanical Properties and Shaping Performance of Heat-Treated Nickel Titanium Rotary Instruments Used in the Single-Length Technique. *Dent. Mater. J.* **2021**, *40*, 743–749. [[CrossRef](#)] [[PubMed](#)]
23. Bürklein, S.; Schäfer, E. Critical Evaluation of Root Canal Transportation by Instrumentation. *Endod. Top.* **2013**, *29*, 110–124. [[CrossRef](#)]
24. Deari, S.; Zehnder, M.; Al-Jadaa, A. Effect of Dentine Cutting Efficiency on the Lateral Force Created by Torque-Controlled Rotary Instruments. *Int. Endod. J.* **2020**, *52*, 237–243. [[CrossRef](#)]

25. Martins, J.N.R.; Silva, E.J.N.L.; Marques, D.; Belladonna, F.; Simões-Carvalho, M.; Vieira, V.T.L.; Antunes, H.S.; Braz Fernandes, F.M.B.; Versiani, M.A. Design, Metallurgical Features, Mechanical Performance and Canal Preparation of Six Reciprocating Instruments. *Int. Endod. J.* **2021**, *54*, 1623–1637. [[CrossRef](#)]
26. Peters, O. Current Challenges and Concepts in the Preparation of Root Canal Systems: A Review. *J. Endod.* **2004**, *30*, 559–567. [[CrossRef](#)]
27. Lim, K.C.; Webber, J. The Validity of Simulated Root Canals for the Investigation of the Prepared Root Canal Shape. *Int. Endod. J.* **1985**, *18*, 240–246. [[CrossRef](#)]
28. Rebeiz, J.; El Hachem, C.; El Osta, N.; Habib, M.; Rebeiz, T.; Zogheib, C.; Kaloustian, M.K. Shaping Ability of a New Heat-Treated Niti System in Continuous Rotation or Reciprocation in Artificial Curved Canals. *Odontology* **2021**, *109*, 792–801. [[CrossRef](#)]
29. Peters, O.; Barbakow, F. Dynamic Torque and Apical Forces of Profile. 04 Rotary Instruments during Preparation of Curved Canals. *Int. Endod. J.* **2002**, *35*, 379–389. [[CrossRef](#)]
30. Pereira, E.S.; Singh, R.; Arias, A.; Peters, O.A. In Vitro Assessment of Torque and Force Generated by Novel ProTaper Next Instruments during Simulated Canal Preparation. *J. Endod.* **2013**, *39*, 1615–1619. [[CrossRef](#)]
31. Bürklein, S.; Poschmann, T.; Schäfer, E. Shaping Ability of Different Nickel-Titanium Systems in Simulated S-shaped Canals with and without Glide Path. *J. Endod.* **2014**, *40*, 1231–1234. [[CrossRef](#)]
32. Özyürek, T.; Yilmaz, K.; Uslu, G. Shaping Ability of Reciproc, WaveOne GOLD, and Hyflex EDM Single-File Systems in Simulated S-Shaped Canals. *J. Endod.* **2017**, *43*, 805–809. [[CrossRef](#)]
33. Weine, F.S.; Kelly, R.F.; Lio, P.J. The Effect of Preparation Procedures on Original Canal Shape and on Apical Foramen Shape. *J. Endod.* **1975**, *1*, 255–262. [[CrossRef](#)]
34. Kwak, S.W.; Shen, Y.; Liu, H.; Kim, H.-C.; Haapasalo, M. Torque Generation of the Endodontic Instruments: A Narrative Review. *Materials* **2022**, *15*, 664. [[CrossRef](#)]
35. Pereira, É.S.J.; Viana, A.; Buono, V.T.L.; Peters, O.; Bahia, M.G.D.A. Behavior of Nickel-Titanium Instruments Manufactured with Different Thermal Treatments. *J. Endod.* **2015**, *41*, 67–71. [[CrossRef](#)]
36. Koch, K.A.; Brave, D.G. Real World Endo: Design Features of Rotary Files and How They Affect Clinical Performance. *Oral Health* **2002**, *92*, 39–49.
37. Versluis, A.; Kim, H.-C.; Lee, W.; Kim, B.-M.; Lee, C.-J. Flexural Stiffness and Stresses in Nickel-Titanium Rotary Files for Various Pitch and Cross-sectional Geometries. *J. Endod.* **2012**, *38*, 1399–1403. [[CrossRef](#)]
38. Peters, O.; Boessler, C.; Zehnder, M. Effect of Liquid and Paste-Type Lubricants on Torque Values during Simulated Rotary Root Canal Instrumentation. *Int. Endod. J.* **2005**, *38*, 223–229. [[CrossRef](#)]
39. Kim, H.-C.; Cheung, G.S.-P.; Lee, C.-J.; Kim, B.-M.; Park, J.-K.; Kang, S.-I. Comparison of Forces Generated during Root Canal Shaping and Residual Stresses of Three Nickel-Titanium Rotary Files by Using a Three-Dimensional Finite-Element Analysis. *J. Endod.* **2008**, *34*, 743–747. [[CrossRef](#)]